Structural Control and Health Monitoring

Investigations on a Particle Filter Algorithm for Crack Identification in Beams from Vibration Measurements

Journal:	*Structural Control and Health Monitoring*
Manuscript ID:	STC-14-0090.R2
Wiley - Manuscript type:	Research Paper
Date Submitted by the Author:	n/a
Complete List of Authors:	Rangaraj, R; Asoke Leyland Technical Center, Pokale, Bharat; IIT Madras, Applied Mechanics Banerjee, Anuradha; IIT Madras, Applied Mechanics Gupta, Sayan; Indian Institute of Technology Madras, Department of Applied Mechanics
Keywords:	Dynamic state estimation, crack, particle filter, Bayesian, health monitoring, vibrations, beam

SCHOLARONE™
Manuscripts
For Review

Investigations on a Particle Filter Algorithm for Crack Identification in Beams from Vibration Measurements

R Rangaraj [1], Bharat Pokale [2], Anuradha Banerjee [2], Sayan Gupta [2] *,

[1] *Asoke Leyland Technical Center, Vellivoyalchavadi, Chennai 600103 India,*
[2] *Department of Applied Mechanics, Indian Institute of Technology Madras, Chennai 600036, India.*

For Peer Review

SUMMARY

This study focusses on crack identification in beams from vibration measurements using principles of dynamic state estimation. The finite element method is used to model the beam with cracked beam elements that account for the presence of an edge crack under near-tip elasto-plastic conditions. The crack size and its location are treated as the variables that are identified using a particle filter algorithm. A parametric study is first carried out with synthetic measurements to numerically analyse the performance of the algorithm. Subsequently, using measurements acquired from physical experiments involving a cantilever beam subjected to arbitrary excitations, the proposed algorithm is used to identify the size and location of crack-like defects. The proposed method do not require measurements of the undamaged beam; hence, can be used for crack identification in beams for which no earlier measurements are available. Copyright © 2000 John Wiley & Sons, Ltd.

KEY WORDS: Dynamic state estimation; crack; particle filter; Bayesian; health monitoring; vibrations; beam

1. Introduction

Identification of crack like defects in beams from ambient vibration measurements is a cost effective method that is commonly used in structural health monitoring applications prone to damage from repetitive loadings [1]. Crack like defects in vibrating beams alter the stiffness and damping properties locally, which in turn, changes the macroscopic beam response characteristics; see [2] for a review. These changes are manifested in terms of the modal parameters, such as, the structure natural frequencies, mode shapes, modal damping ratios etc. Techniques available in the literature, for crack identification from vibration measurements are therefore primarily modal based approaches. The underlying principle of these methods lie in relating the changes in the modal characteristics to location and severity of cracks. This can be addressed as a forward problem or as an inverse problem [3]. In the forward approach, investigations have been carried out to study the changes that result due to the presence of

*Correspondence to: Sayan Gupta, Department of Applied Mechanics, Indian Institute of Technology Madras, Chennai 600036, India. E-mail: sayan@iitm.ac.in

cracks at known locations [4–7]. In the inverse approach, the location and the size of the cracks are estimated by relating the crack parameters with the changes in the modal characteristics, in conjunction with optimization techniques; see for example [8–19]. Typically, these methods focus on developing equations that relate the unknown parameters, such as, crack size, crack locations, local flexibility coefficients etc., with changes in the structure natural frequencies, mode shapes and modal damping ratios. This usually leads to a system of overdetermined equations and estimates of the crack sizes and their locations are obtained by application of techniques, such as, rank-ordering methods, regularization and error minimization methods, least square approaches etc. Studies on using the changes in the antiresonance peaks in the frequency response functions have also been carried out to locate cracks [20–22]. Alternative methods that use modal parameters for crack detection include optimization approaches in conjunction with perturbation methods [23] and wavelet analysis [24, 25].

Time domain based studies using iterative approaches for locating and estimating the severity of damage from vibration measurements have been discussed in [26–30]. These studies typically introduce the damage into the numerical model either through an unknown variable or a function with unknown parameters. Subsequently, these unknown quantities are estimated through an iterative procedure applied on available response measurements. Unlike modal analysis based methods which are primarily applicable to linear systems, these methods are applicable in nonlinear systems [28, 29] as well as when measurements are noisy [30, 31]. However, inverse methods using deterministic models lack robustness due to the unknown and unavoidable errors that enter the analysis due to the inevitable inaccuracies in mathematical modelling and data acquisition. These errors enter the inverse analysis in the form of noise which need to be appropriately taken into account.

The robustness of inverse methods can be improved by explicit modeling of the uncertainties (*i.e.*, noise) using a probabilistic approach. This has led to adopting Bayesian filtering frameworks in the damage detection algorithms. The focus in these methods is not on identifying the exact location and sizes of the damage, but on defining their corresponding probability density functions (pdf)s and estimating their most probable values, conditioned on the available measurements. A set of variables are defined for the system and/or damage parameters to be identified; these are modeled as random variables with an assumed pdf. A vector of realizations for these random variables is simulated in the computer having the specified probabilistic properties. Corresponding to each realization for the system parameters, a mathematical model is used to predict the structure response for a particular time instant. Using Bayesian theories, the distributions of the unknown parameters in the mathematical model are subsequently updated by comparing the predictions with the actual measurement at that time instant. The updated pdf of the parameters are used to resample realizations for the next response measurement instant. This procedure is carried out recursively till convergence is achieved in the prediction of the system parameters. Closed form analytical expressions have been developed when the system equations are linear, the noise in the system are modeled as Gaussian variables and the parameters to be estimated constitute the state vector, leading to the well known Kalman filter [32]. When the parameters to be identified do not belong to the state vector, the equations for the parameters being identified become nonlinear which rule out the direct application of the Kalman filter. This has led to the development of Kalman filter based algorithms for damage detection [33–36] which rely on linearizing the equations in conjunction with the traditional form of Kalman filtering techniques. The robustness of these variants of the Kalman filter are, however, limited and depend on the extent of the nonlinearity

Copyright © 2000 John Wiley & Sons, Ltd.

Prepared using stcauth.cls

For Peer Review

associated with the model and the measurement equations and the assumed distribution of the unknowns associated with the system.

The advent of cheap computing facilities in recent times has led to the focus on the development of inverse methods, such as the particle filter based methods, which are more robust irrespective of the nonlinearities and the non-Gaussianities associated with the system. These methods rely on using Monte Carlo simulations and numerically integrating the associated equations rather than seeking analytical approximations for the conditional pdf of the unknown parameters. Thus, these methods place no restrictions on the form of the equations or the distributions of the unknown parameters and noise. Here, the system parameters to be identified are treated as the state variables and the measurements that are used could from a combination of static and/or dynamic tests [37].

The focus of the present study is on the development of a particle filtering methodology, for identifying crack like defects in structural systems from vibration measurements. The crux of the proposed method lies in adopting a finite element framework for modeling the crack induced damaged beam and formulating the inverse problem in terms of the damage variables only, with all other state variables being treated as internal variables. Subsequently, the Bayesian particle filtering is carried out in the reduced space spanned by the vector of unknown damage parameters. The novel feature of the proposed method lies not only in quantifying the most likely size of a predominant crack like defect from vibration measurements, but also to estimate the most likely location of the crack. Unlike most existing studies, this is carried out without the need for having measurements of the undamaged beam.

2. Problem Statement

A cantilever beam of length L, having a crack like defect of length a situated at a distance l from the fixed end, is considered; see Fig. 1. The cross-section of the beam is assumed to be rectangular having dimensions $b \times d$. The crack like defect is assumed to be on the surface,

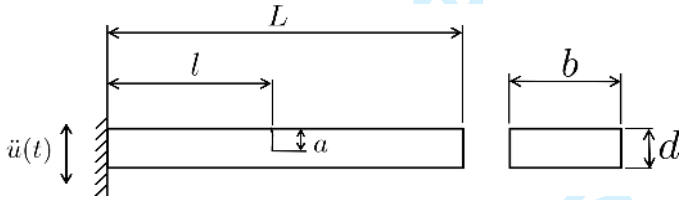

Figure 1: Schematic diagram of a cantilever beam with a crack.

is a through crack along the breadth of the beam and is assumed to remain always open. The excitations are assumed to be through support motion in the numerical examples. The vibration response at the tip of the beam is measured. The focus is therefore on identifying from vibration measurements, (1) the location in the beam where there is a local reduction in the stiffness properties, (2) the magnitude by which the stiffness decreases locally, and (3) relating this stiffness change to the size of a crack, using particle filtering. The identification strategy needs to address the above three-fold problem. As can be seen from the schematic diagram in Fig. 1, this implies that two parameters need to be identified, (a) l - the location

Copyright © 2000 John Wiley & Sons, Ltd.

Prepared using stcauth.cls

of the fatigue crack, and (b) the size of the crack denoted by a.

The finite element (FE) discretised equations of motion for the beam are

$$\mathbf{M}\ddot{\mathbf{y}}(t) + \mathbf{C}\dot{\mathbf{y}}(t) + \mathbf{K}\mathbf{y}(t) = -\mathbf{M}\mathbf{1}\ddot{u}(t), \tag{1}$$

where, $\mathbf{M}$, $\mathbf{C}$ and $\mathbf{K}$ are respectively, the mass, damping and stiffness matrices of dimensions $n \times n$, $\mathbf{y}(t)$, $\dot{\mathbf{y}}(t)$ and $\ddot{\mathbf{y}}(t)$ are the vectors of nodal displacements, velocities and accelerations of dimensions $n \times 1$, $\ddot{u}(t)$ is the nodal ground accelerations in the transverse direction only and $\mathbf{1}$ is the vector of participation factors, consisting of 1 corresponding to the transverse support node and 0 at all the other nodes. Even though a cantilever beam is being considered in this study, the methodology being presented here is not specific to cantilever beams only or when the excitations are through support motions.

2.1. Modeling the Local Flexibility due to Cracks

The crux of the problem lies in using a FE model for the cracked beam, which captures the effects of cracks without too complicated FE meshing. This can be achieved using the FE cracked beam element developed in [38]. The element consists of three segments - (a) an undamaged beam segment to the left of the crack, (b) a similar beam segment to the right of the crack and (c) the crack. The left and the right segments in the crack are assumed to be of equal length, $L/2$, where L is the length of the cracked beam element and the crack is modeled by a massless rotational spring k_θ having zero dimensions. The cracked beam element is assumed to consist of two nodes, located at the extremities of the cracked beam, with each node having a translational and a rotational degree-of-freedom. The stiffness of the rotational spring, k_θ, is modeled, such that, the local flexibility due to the crack is considered. The local flexibility c is the inverse of the local stiffness k_θ and is dependent on the crack size. Using theories of elasto-plastic fracture mechanics, the local flexibility c can be related to the fatigue crack size a [38]. Here, the effect of the plastic zone that appear in front of crack tips which provide additional flexibilities in the material is considered; see Fig. 2 for a schematic diagram. The radius of the plastic zone, r_p, around the crack tip, is given as [39] $r_p = (K_{I_p}/\sigma_Y)^2/(2\pi)$,

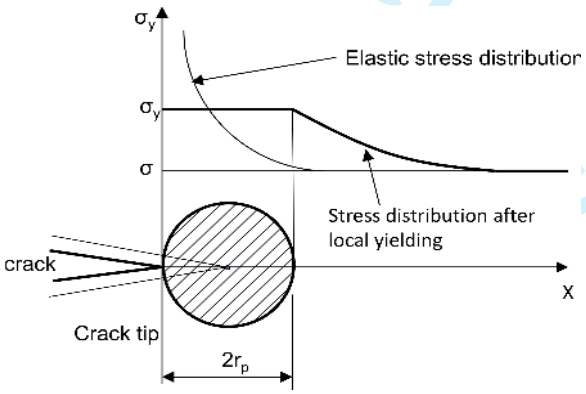

Figure 2: Plastic zone around the crack tip

where, σ_Y is the material yield strength and K_{I_p} is the elasto-plastic stress intensity factor

Copyright © 2000 John Wiley & Sons, Ltd.

Prepared using stcauth.cls

given by

$$K_{I_p} = K_I[1 + \sigma_M^2 \zeta^2/(2\pi\sigma_Y^2)]^{0.5}. \tag{2}$$

Here, K_I is the elastic stress intensity factor, σ_M is the applied stress due to bending moment, M, and η is a correction function which incorporates the effects of the structure component and the crack geometries. For a beam of rectangular cross-sections with breadth, b and depth, d, the correction function is given as

$$\zeta = \sqrt{\frac{\tan(\kappa)}{\kappa}}\left(\frac{0.923 + 0.199[1 - \sin(\kappa)]^4}{\cos(\kappa)}\right), \tag{3}$$

where, $\kappa = \pi a/2d$ and $K_I = 6M/bd^2$. The general expression for finding the local flexibility due to a crack [40] is $c_{ij} = \partial^2/\partial F_i \partial F_j[\int_{\mathcal{A}} J_c \, \mathrm{d}\mathcal{A}]$, where, F_i is the applied generalized force at the i-th location, $\mathcal{A}$ is the area of the cross-section and assuming stress is generated due to bending only, J_c is the strain energy density function given by $J_c = K_{I_{p_i}}^2/E$. Assuming a through crack and that plane stress conditions are applicable, it can be shown that

$$c = \frac{72}{Ebd^2}\int_0^{\bar{a}_k} \zeta(\bar{a})^2 \, \bar{a} \, \mathrm{d}\bar{a} + \frac{216}{E\pi bd^2}\left(\frac{\sigma_M}{\sigma_Y}\right)^2 \int_0^{\bar{a}_k} \zeta(\bar{a})^4 \, \bar{a} \, \mathrm{d}\bar{a}, \tag{4}$$

where, $\zeta \equiv \zeta(a)$ is as given in Eq. (3), a and a_k denote the crack size, and $\bar{a} = a/d$ and $\bar{a}_k = a_k/d$ are the non-dimensionalized size of the crack, expressed as a ratio in terms of the beam depth d. Thus, Eq.(4) provides a relationship between the crack size and the local flexibility introduced in the beam due to the presence of a crack. It has been shown in [38] that the stiffness matrix is of the form

$$\mathbf{K} = EI\begin{bmatrix} \frac{12}{L^3} & \frac{6}{L^3} & -\frac{12}{L^3} & \frac{6}{L^2} \\ & \frac{4L^2+6L\psi+3\psi^2}{L(L+\psi)^2} & -\frac{6}{L^2} & \frac{2L^2+6L\psi+3\psi^2}{L(L+\psi)^2} \\ & & \frac{12}{L^3} & -\frac{6}{L^2} \\ \text{sym} & & & \frac{4L^2+6L\psi+3\psi^2}{L(L+\psi)^2} \end{bmatrix} \tag{5}$$

and the mass matrix is given by

$$\mathbf{M} = \left(\frac{\rho AL}{420}\right)\mathbf{M_1} + \left(\rho JL\right)\mathbf{M_2}, \tag{6}$$

$$\mathbf{M_1} = \begin{bmatrix} 156 & \frac{L^2(88L+123\psi)}{4(L+\psi)} & 54 & -\frac{L^2(52L+87\psi)}{4(L+\psi)} \\ & \frac{L^3(64L^2+191L\psi+148\psi^2)}{16(L+\psi)^2} & -\frac{L^2(52L+87\psi)}{4(L+\psi)} & \frac{3L^3(16L^2+53L\psi+44\psi^2)}{16(L+\psi)^2} \\ & & 156 & -\frac{L^2(88L+123\psi)}{4(L+\psi)} \\ \text{sym} & & & \frac{L^3(64L^2+191L\psi+148\psi^2)}{16(L+\psi)^2} \end{bmatrix}, \tag{7}$$

Copyright © 2000 John Wiley & Sons, Ltd.

Prepared using stcauth.cls

For Peer Review

$$\mathbf{M_2} = \begin{bmatrix} \frac{6}{5L^2} & \frac{1}{10L} & -\frac{6}{5L^2} & \frac{1}{10L} \\ & \frac{L(8L^2+21L\psi+18\psi^2)}{60(L+\psi)^2} & -\frac{1}{10L} & -\frac{L(8L^2+21L\psi+18\psi^2)}{60(L+\psi)^2} \\ & & \frac{6}{5L^2} & -\frac{1}{10L} \\ \text{sym} & & & \frac{L(8L^2+21L\psi+18\psi^2)}{60(L+\psi)^2} \end{bmatrix}. \quad (8)$$

Here, $\psi = EIc$. In the absence of any crack, $c = 0$ and the resultant stiffness and the mass matrices become identical to the Euler-Bernoulli beam matrices.

It is quite clear that the equations involving the elasto-plastic model for the crack growth are nonlinear. On the other hand, the governing equations of motion in Eq. (1) are assumed to be linear. This apparent contradiction can be explained by the fact that the elasto-plastic model takes into account the localized behaviour of the material near the crack tip and is more accurate when relating the loss of local flexibilities to crack sizes. However, the effects of the crack on the stress field at locations away from the crack tip are negligible. This is observed from the macroscopic linear behaviour of the stress-strain curves obtained from experiments and verified by numerical experiments on cracked specimens for loadings below a critical threshold; see Fig.4 in [41]. The equations of motion in Eq. (1) represents the macroscopic behaviour of the vibrating structure which are primarily governed by the macro-stress fields; the localised effects due to micro-defects do not affect the macroscopic behaviour unless the loading is significant or the cracks are assumed to propagate during the measurements. Thus, under these assumptions, the use of linear equations of motion for modelling the macroscopic behaviour is not inconsistent.

For Peer Review

2.2. Parameter Identification

The beam is discretized using S cracked beam elements with c_j associated with each element being treated as the unknown parameters to be identified. Here, it is assumed that the FE discretisation is carried out in a manner such that there exists only a single crack within an element. This enables FE modelling using the cracked beam element discussed in the previous section. For elements without a crack, the successful implementation of the identification algorithm should lead to c_j converging to zero. Collectively, these parameters are represented through the S-dimensional vector $\boldsymbol{\theta}$. An approximation for the location of the crack can be obtained from identifying the i-th elemental location corresponding to which $c_i \neq 0$ and an estimate of the size of the crack can be obtained from Eq. (4). Though the equations of motion are linear, the beam response is a nonlinear function of $\boldsymbol{\theta}$. This rules out the direct use of the Kalman filter algorithm. Instead, we develop a variant of the particle filter algorithm to obtain estimates of $\boldsymbol{\theta}$ from vibration measurements. This is discussed in the following sections.

Copyright © 2000 John Wiley & Sons, Ltd.

Prepared using stcauth.cls

3. Filtering

3.1. Dynamic state estimation

Estimates for the system parameters can be obtained from measurement data using the principles of dynamic state estimation. This involves rewriting the governing equations in the first order form and when recast into the discrete recursive format, is expressed as $\mathbf{Z}_{k+1} = \mathbf{f}_k(\mathbf{Z}_k, \boldsymbol{\theta}_k)$, where, $\mathbf{Z}_k$ denotes the $2n$-dimensional state vector at time step $t = t_k$ for the system when the FE model is discretized into n degrees of freedom, $\boldsymbol{\theta}_k$ denotes the q-dimensional vector of system parameters at t_k and $\mathbf{f}_k(\cdot)$ is the form of the functional relationship at t_k that relates $\mathbf{Z}_k$ and $\mathbf{Z}_{k+1}$.Considering an augmented state vector $\mathbf{X}_k = [\mathbf{Z}_k \;\; \boldsymbol{\theta}_k]^T$ of dimension $2n + q$, where the superscript T denotes matrix transpose, the recursive relation between the state vector can be rewritten as

$$\mathbf{X}_{k+1} = \mathbf{g}_k(\mathbf{X}_k, \mathbf{w}_k). \tag{9}$$

where, $\mathbf{w}_k \in \Re^m$ is a sequence of zero mean i.i.d. random variables representing the discretized m-dimensional vector of white noise processes that take into account the modeling uncertainties and $\mathbf{g}_k(\cdot)$ is a nonlinear system transition function, such that, $\mathbf{g}_k(\cdot) : \Re^{2n+q} \times \Re^m \rightarrow \Re^{2n+q}$. Equation (9) is known as the model equation. Here, no assumptions have been made on the noise $\mathbf{w}_k$ being additive or multiplicative, or its pdf. The relationship between the measurements and the state variables, can be mathematically expressed through the measurement equation

$$\mathbf{Y}_k = \mathbf{h}_k(\mathbf{X}_k, \mathbf{v}_k), \tag{10}$$

where, $\mathbf{Y}_k \in \Re^p$ is a p-dimensional vector of measurements, $\mathbf{v}_k \in \Re^r$ is a $r-$ dimensional vector of a sequence of zero-mean, i.i.d. random variables and $\mathbf{h}_k(\cdot)$ is a nonlinear function that relates the measurements to the system state, such that, $\mathbf{h}_k(\cdot) : \Re^{2n+q} \times \Re^r \rightarrow \Re^p$. Here, the sequence of i.i.d. random variables, $\mathbf{v}_k$, represent the discretized form of a vector of white noise processes which take into account all the uncertainties associated in relating the measurements $\mathbf{Y}_k$ with the state $\mathbf{X}_k$.

Filtering involves using Eqs. (9-10) to estimate $\mathbf{X}_k$ from available measurement data sets $\mathbf{D}_k = \{\mathbf{Y}_1, \mathbf{Y}_2, \ldots, \mathbf{Y}_k\}$ using Bayesian principles [42]. Since both $\mathbf{X}_k$ and $\mathbf{Y}_k$ are corrupted by noise, complete characterization of $\mathbf{X}_k$ is possible only in terms of $p(\mathbf{X}_k|\mathbf{D}_k)$ - the pdf of $\mathbf{X}_k$, conditioned on available measurements $\mathbf{D}_k$. We denote $p(\mathbf{X}_k|\mathbf{D}_{k-1})$ as the *a priori* pdf - the estimate of the pdf of state $\mathbf{X}_k$ based on measurements $\mathbf{D}_{k-1}$, and $p(\mathbf{X}_k|\mathbf{D}_k)$ to be the *posteriori* pdf of $\mathbf{X}_k$ based on measurements $\mathbf{D}_k$. Further, it is assumed that $p(\mathbf{X}_1|\mathbf{D}_0) \equiv p(\mathbf{X}_1)$ is known. This assumption is not restrictive as any errors in assuming $p(\mathbf{X}_1)$ can be taken care through the model noise in subsequent steps.

Assuming $p(\mathbf{X}_{k-1}|\mathbf{D}_{k-1})$ to be available at t_{k-1}, the prediction equation can be expressed as

$$p(\mathbf{X}_k|\mathbf{D}_{k-1}) = \int p(\mathbf{X}_k|\mathbf{X}_{k-1}) p(\mathbf{X}_{k-1}|\mathbf{D}_{k-1}) \; \mathrm{d}\mathbf{X}_{k-1}. \tag{11}$$

Here, $p(\mathbf{X}_k|\mathbf{X}_{k-1})$ is the pdf of the state evolution and expressed as

$$p(\mathbf{X}_k|\mathbf{X}_{k-1}) = \int p(\mathbf{X}_k|\mathbf{X}_{k-1}, \mathbf{w}_{k-1}) p(\mathbf{w}_{k-1}|\mathbf{X}_{k-1}) \; \mathrm{d}\mathbf{w}_{k-1}. \tag{12}$$

As $\mathbf{w}_k$ is independent of the state, $p(\mathbf{w}_{k-1}|\mathbf{X}_{k-1}) \equiv p(\mathbf{w}_{k-1})$. From Eq. (9), it follows that if $\mathbf{X}_{k-1}$ and $\mathbf{w}_{k-1}$ are known, then $\mathbf{X}_k$ can be expressed in terms of $\mathbf{X}_{k-1}$ and $\mathbf{w}_{k-1}$

Copyright © 2000 John Wiley & Sons, Ltd.

Prepared using stcauth.cls

For Peer Review

deterministically, and can be written as

$$p((\mathbf{X}_k|\mathbf{X}_{k-1}, \mathbf{w}_{k-1}) \equiv \delta(\mathbf{X}_k - \mathbf{g}_{k-1}(\mathbf{X}_{k-1}, \mathbf{w}_{k-1})), \tag{13}$$

where, $\delta(\cdot)$ is the Dirac-delta function. Substituting in Eq. (12), we get

$$p(\mathbf{X}_k|\mathbf{X}_{k-1}) = \int \delta(\mathbf{X}_k - \mathbf{g}_{k-1}(\mathbf{X}_{k-1}, \mathbf{w}_{k-1}))p(\mathbf{w}_{k-1})\ \mathrm{d}\mathbf{w}_{k-1}. \tag{14}$$

Once measurement $\mathbf{Y}_k$ is available at time step k, the prediction can be updated using the Bayesian relation

$$p(\mathbf{X}_k|\mathbf{D}_k) = \frac{p(\mathbf{Y}_k|\mathbf{X}_k)p(\mathbf{X}_k|\mathbf{D}_{k-1})}{p(\mathbf{Y}_k|\mathbf{D}_{k-1})}, \tag{15}$$

where, the normalizing denominator is given by

$$p(\mathbf{Y}_k|\mathbf{D}_{k-1}) = \int p(\mathbf{Y}_k|\mathbf{X}_k)p(\mathbf{X}_k|\mathbf{D}_{k-1})\ \mathrm{d}\mathbf{X}_k, \tag{16}$$

with, $p(\mathbf{X}_k|\mathbf{D}_{k-1})$ available from Eq. (11). The unknown term in Eq. (15) is $p(\mathbf{Y}_k|\mathbf{X}_k)$and can be expressed as

$$p(\mathbf{Y}_k|\mathbf{X}_k) \quad = \int \delta(\mathbf{y}_k - \mathbf{h}_k(\mathbf{X}_k, \mathbf{v}_k))p(\mathbf{v}_k)\ \mathrm{d}\mathbf{v}_k. \tag{17}$$

Here, $p(\mathbf{Y}_k|\mathbf{X}_k, \mathbf{v}_k)$ is represented as the Dirac-delta function because if $\mathbf{X}_k$ and $\mathbf{v}_k$ is known, then the measurement $\mathbf{Y}_k$ is available deterministically from Eq. (10). Eqs. (11-17) constitute the formal solution of the Bayesian recursive estimation problem. As estimating $p(\mathbf{X}_k|\mathbf{D}_k)$ is not easy, it is simpler to estimate the first two moments at each time step, given by

$$\mathbf{a}_{k|k} \quad = \int \mathbf{X}_k\ p(\mathbf{X}_k|\mathbf{D}_k)\ \mathrm{d}\mathbf{X}_k, \tag{18}$$

$$\mathbf{\Sigma}_{k|k} \quad = \int (\mathbf{X}_k - \mathbf{a}_{k|k})^T(\mathbf{X}_k - \mathbf{a}_{k|k})\ p(\mathbf{X}_k|\mathbf{D}_k)\ \mathrm{d}\mathbf{X}_k. \tag{19}$$

Here, $\mathbf{a}_{k|k}$ is the mean and $\mathbf{\Sigma}_{k|k}$ is the variance and gives an indication of the error associated with the predictions.

A crucial step in the filtering is the evaluation of the multi-dimensional integrals spanned by the vector $\mathbf{X}_k$; see Eqs. (11-19). Closed form expressions for these integrals are available only if $\mathbf{f}_k(\,\cdot\,)$ and $\mathbf{h}_k(\,\cdot\,)$ are linear and the noise terms, $\mathbf{w}_k$ and $\mathbf{v}_k$ are Gaussian and additive, leading to the well known Kalman filter. For the crack identification problem being considered in this paper, $\mathbf{f}_k(\,\cdot\,)$ and $\mathbf{h}_k(\,\cdot\,)$ are nonlinear. Rather than using variants of the Kalman filter which are based on linearization of the model and the measurement equations and hence are prone to errors, this study uses Monte Carlo simulations for obtaining approximations for these multi-dimensional integrals. These methods are typically referred to as particle filters. More details of the particle filter used in this study is discussed next.

3.2. The Bootstrap Particle Filter

In this study, we use a variant of the bootstrap particle filter proposed in [42]. The method of augmenting the state vector $\mathbf{Z}_k$ with the system parameters $\boldsymbol{\theta}_k$ increases the vector size $\mathbf{X}_k = [\mathbf{Z}_k, \boldsymbol{\theta}_k]$ on which the filtering is to be carried out, which in turn, increases the

Copyright © 2000 John Wiley & Sons, Ltd.

Prepared using stcauth.cls

For Peer Review

computational costs. This problem was circumvented in [43] by rewriting the model and the measurement equations only in terms of $\boldsymbol{\theta}_k$ - the parameters that are to be identified; the state variables $\mathbf{Z}_k$ were considered to be internal variables. Adopting the same principles here and assuming that (a) the vibration measurements are acquired for only short durations of time, and (b) there is no growth in the crack size during this small time interval, the model equations are expressed as

$$\frac{\mathrm{d}\boldsymbol{\theta}_j}{\mathrm{d}t} = 0; \quad \boldsymbol{\theta}_j(0) = \boldsymbol{\theta}_{0_j}, \qquad j = 1, \ldots, n, \tag{20}$$

where, j denotes the j-th parameter in the vector $\boldsymbol{\theta}$ and $\boldsymbol{\theta}_0$ is the vector of initial conditions. Since Eq.(20) implies that the system parameters remain invariant, it is obvious that in the discretized recursive format, $\boldsymbol{\theta}_{k+1} = \boldsymbol{\theta}_k$. Adding a noise leads to the model equation being written as

$$\boldsymbol{\theta}_{k+1} = \boldsymbol{\theta}_k + \mathbf{w}_k. \tag{21}$$

Here, $\mathbf{w}_k \in \Re^q$ denotes a sequence of i.i.d. random variables with density $p(\boldsymbol{\theta})$. It is further assumed that $\boldsymbol{\theta}_0$ are also uncertain and are modeled as a vector of random variables having a pdf $p(\boldsymbol{\theta}_0)$. Noise $\mathbf{w}_k$ is artificial and does not have any physical significance. The reasons for adding $\mathbf{w}_k$ will be explained later.

The measurement equation is expressed in terms of $\boldsymbol{\theta}_k$ and is written as

$$\mathbf{Y}_k = \mathbf{h}_k(\boldsymbol{\theta}_k) + \mathbf{v}_k, \tag{22}$$

where, $\mathbf{h}_k(\,\cdot\,)$ is the function that relates the system parameters $\boldsymbol{\theta}_k$ to the measurement vector $\mathbf{Y}_k$, at time step t_k. Here, $\mathbf{v}_k$ is a sequence of i.i.d. random variables with pdf $p(\mathbf{v}_k)$ that models all sources of errors and uncertainties in modeling the relationship between the measurements, $\mathbf{Y}_k$, and the system parameters $\boldsymbol{\theta}_k$. Here, $\mathbf{v}_k$ represent both modelling and measurement errors.

Eqs. (21-22) together constitute the model and the measurement equations on which the particle filter algorithm needs to be applied. In formulating the problem in this manner, the model equation is linear while the measurement equation is nonlinear. Moreover, the functional relationship $\mathbf{h}_k(\,\cdot\,)$ is usually available only in an implicit form. However, this is not a problem as the integrals in the Bayesian updating procedure are evaluated using Monte Carlo simulations. The advantage in the proposed approach lies in being able to reduce the dimension of the state vector being identified to the dimension of $\boldsymbol{\theta}$. This can be considerably advantageous computationally as application of the particle filtering on a complex structural system modeled using FEM and having thousands of nodes, may require filtering only on a small dimension equal to the number of parameters to be identified.

3.3. The Algorithm

The steps involved in application of the bootstrap particle filter algorithm are as follows:

1. For $k = 0$, simulate N samples for $\boldsymbol{\theta}_0$ from the assumed pdf $p(\boldsymbol{\theta}_0)$.
2. For $k = 1$, calculate the prior predictions for the state, in this case denoted by $\boldsymbol{\theta}_k^* = \boldsymbol{\theta}_{k-1}$, as the system parameters are assumed to be invariant for the duration of the measurements.
3. Once the measurements at the k -th instant are available, the likelihood corresponding to all the samples $\{\boldsymbol{\theta}_{k_j}^*\}_{j=1}^N$ are evaluated as $\mathcal{L}(\mathbf{Y}_k|\boldsymbol{\theta}_{k_j}^*) = \mathbf{Y}_k - \mathbf{h}_k(\boldsymbol{\theta}_k^*)$.

Copyright © 2000 John Wiley & Sons, Ltd.

Prepared using stcauth.cls

For Peer Review

4. An approximation for $p(\mathbf{Y}_k|\boldsymbol{\theta}^*_{k_j})$ is obtained by normalizing the likelihood function as

$$q_j = \frac{\mathcal{L}(\mathbf{Y}_k|\boldsymbol{\theta}^*_{k_j})}{\sum_{j=1}^{N}\mathcal{L}(\mathbf{Y}_k|\boldsymbol{\theta}^*_{k_j})}. \tag{23}$$

5. The discrete probability mass function for the next iterate is defined as

$$P[\boldsymbol{\theta}_{k_j} = \boldsymbol{\theta}^*_k] = q_j. \tag{24}$$

6. From the discrete probability mass function in Eq. (24), a new set of N samples of $\boldsymbol{\theta}_k$ are generated which are the posterior estimates of $\boldsymbol{\theta}_k$.
7. The mean of the estimates are obtained as

$$\bar{\boldsymbol{\theta}}_{k|k} = \frac{1}{N}\sum_{j=1}^{N}\boldsymbol{\theta}_{k_j}. \tag{25}$$

The corresponding standard deviation of the estimate is calculated as

$$\bar{\boldsymbol{\sigma}}_{k|k} = \sqrt{\frac{1}{N-1}\sum_{j=1}^{N}(\boldsymbol{\theta}_{k_j} - \bar{\boldsymbol{\theta}}_{k|k})^T(\boldsymbol{\theta}_{k_j} - \bar{\boldsymbol{\theta}}_{k|k})}. \tag{26}$$

8. The above steps are repeated by setting $k = k + 1$. In this way, the filtering is carried out for the entire available time history of measurements.

The above algorithm requires N evaluations of the structure analysis code at each time step. Thus, if there are M measurements available, and a filtering is carried out at each of these M measurement data points, the number of structure evaluations required is $N \times M$. Of all the samples for $\boldsymbol{\theta}^*_k$, the ones which lead to response which are closest to the measured values are likely to be nearer the actual parameters. Thus, one generates a vector of prior estimates $\{\boldsymbol{\theta}^*_{k_j}\}_{j=1}^N$ and evaluates the likelihood function $\mathcal{L}(\mathbf{Y}_k|\boldsymbol{\theta}^*_{k_j})$. Subsequently, the probability mass function is defined as in Eq. (24). Next, samples are drawn from this mass function. Obviously, of the N samples generated, more samples would be drawn corresponding to samples having greater weights q_i. Following the bootstrap procedure, in subsequent iterations the population of samples would be limited to the samples that have been generated at $k = 0$. This leads to the following difficulties: (a) after a few iterations, all the samples generated for $\boldsymbol{\theta}_{k+1}$ would be identical leading to a degenerate condition resulting in the breakdown of the filtering procedure, and (b) the accuracy of the system parameter estimates would depend on the closeness of the initial set of variables generated for $\boldsymbol{\theta}_0$ to the actual system parameters. To prevent such degeneracies, artificial noise $\mathbf{w}_k$ is added to the posterior estimates, $\boldsymbol{\theta}_k$, at each time step. This ensures that the samples that are generated from the probability mass function, at each time step, are different from the original set of samples that were generated at $k = 0$. Obviously, the accuracy of the algorithm would depend on the choice of $p(\mathbf{w}_k)$. It is reasonable to assume that $\mathbf{w}_k$ is independent of time as well as $\boldsymbol{\theta}_k$ and $\mathbf{v}_k$. Usually, a Gaussian model for $p(\mathbf{w}_k)$ can be assumed with zero mean and a small variance. The variance should be small so that the population of samples generated from the probability mass function are "slightly" different from the samples that have been identified as having higher likelihoods. Also, this enables generation of a larger number of samples around the most likely sample, leading to the possibility of achieving greater accuracy levels.

Copyright © 2000 John Wiley & Sons, Ltd.

Prepared using stcauth.cls

For Peer Review

The next question that needs to be addressed is the choice of the pdf $p(\boldsymbol{\theta}_0)$. Usually, if one has prior information about the likely values of the parameters, one can decide on a Gaussian pdf centered about the likely values. However, in the absence of any information, one can consider $p(\boldsymbol{\theta}_0)$ to be uniformly distributed in a range $[\boldsymbol{\theta}_l, \boldsymbol{\theta}_u]$, where, the subscripts l and u, respectively denote the lower and upper bounds and can be chosen based from physical considerations. In the numerical calculations presented in the next section, it will be shown that in estimation of system parameters, the proposed methodology is insensitive to the errors in choice of the range for $\boldsymbol{\theta}$.

4. Numerical Examples and Discussions

A cantilever beam of length 150 mm and cross-sectional dimensions 10×3 mm, is considered. The material is assumed to be aluminium having mass density 2700 kg/m^3 and modulus of elasticity 75×10^9 N/mm^2. The first five natural frequencies, calculated analytically, are 17.94, 657.25, 3970.40, 6281.60 and 13023.00 rad/s respectively. Next, the beam is FE discretized using 5 Euler-Bernoulli beam elements. An eigenvalue analysis of the 5-element undamaged discretized model leads to natural frequencies that are identical to the analytical predictions indicating that the suitability of the 5-element FE model. Any discretisation errors are assumed to be small enough to be addressed through the uncertainty parameters in the particle filter algorithm. For the time domain analysis, a Rayleigh proportional damping model has been considered. More details on the FE model and its validation are available in [44].

The beam is next modeled using P cracked beam finite elements. The supports are assumed to be subjected to harmonic transverse accelerations $\ddot{u}(t)$ with frequency 20 rad/s and are implemented in the FE model using the large mass concept. The resultant set of coupled differential equations are recast in the first order form and are numerically integrated using the β-Newmark algorithm so that the integration time steps are equal to the data acquisition sampling rate. The measurements, in the form of accelerations, are obtained synthetically by solving the forward problem and adding noise to the response. Since a 5 element model is used in the computations, the dimension of $\boldsymbol{\theta}$ is 5. The crack is assumed to be at the center of the beam and the response measurements are taken at the free end. The size of the cracks are expressed in terms of a non-dimensional variable $\bar{a} = a/h$. Usually for cracks $\bar{a} > 0.25$, deterministic methods which use changes in natural frequencies and mode shapes are sufficiently accurate. Here, the efficiency of the algorithm in identifying $\bar{a} \leq 0.2$ are investigated.

4.1. Identifying the crack size at known location

First, it is assumed that the location of the crack size is known with only the crack size $\bar{a}$ to be identified. Thus, the dimension of $\boldsymbol{\theta}$ is one. The number of particles N is taken to be 1000. A parametric study is carried out to check for the robustness of the method by considering three cases where the crack sizes $\bar{a}$ were assumed to be 0.2, 0.05 and 0.025. In the absence of any information, the initial pdf $p(\boldsymbol{\theta}_0)$ is assumed to be uniformly distributed in $[0.05, 0.5]$ for all the cases. Note that the actual crack size lies within this band only in the first two cases. Figures 3-4 show that the estimates of the mean crack size converge correctly quite fast. An inspection of the standard deviation of the estimates show that they tend towards zero

Copyright © 2000 John Wiley & Sons, Ltd.

Prepared using stcauth.cls

For Peer Review

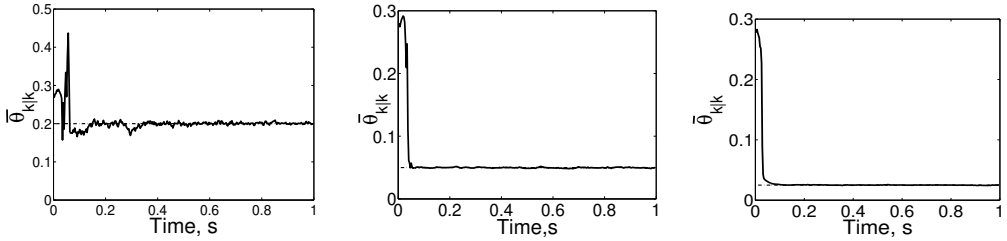

(a) $\bar{a} = 0.2$ (b) $\bar{a} = 0.05$ (c) $\bar{a} = 0.025$

Figure 3: Case Study 1: Mean estimates of $\bar{a}$.

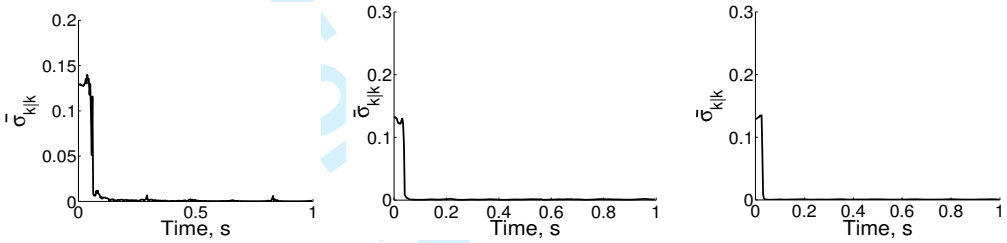

(a) $\bar{a} = 0.2$ (b) $\bar{a} = 0.05$ (c) $\bar{a} = 0.025$

Figure 4: Case Study 1: Standard deviation estimates of $\bar{a}$.

indicating convergence in the estimates. The mean crack estimates in the above figures reveal that for smaller crack sizes, the statistical convergence is quicker. However, the algorithm was unable to accurately estimate the crack size when $\bar{a} = 0.01$. This gives an indication of the lower limit of the efficiency of the method.

Since the computational cost is proportional to N, the performance of the algorithm with smaller N is next investigated. Assuming $N = 50$, it has been observed that the convergence is slower and not to desired levels. To improve the accuracy of the identification with $N = 50$ particles, global iterations are carried out. Global iteration involves the following steps: (a) Using the particle filtering algorithm outlined in steps 1-7; (b) Once the the filtering is carried out for the entire duration of measurements, the steps are repeated from $k = 0$ once again. However, here, the initial distribution of the parameters to be identified is assumed to be the probability mass function obtained at the end of the filtering in step (a). This constitutes a global iteration; (c) steps (a) and (b) are repeated till convergence is achieved. Fig. 5 show how the estimates for the $\bar{\theta}_{k|k}$ varies with global iterations. An inspection of the y-axes in Fig.5 reveal that good convergence is achieved within the first three global iterations. If there are M data points, using 50 particles and with three global iterations implies $M \times 50 \times 3$ solutions of the forward problem. This is in contrast to $M \times 1000$ solutions of the forward problem when $N = 1000$. Thus, significant savings in computational costs is achieved by using smaller N in conjunction with global iterations. More importantly, using global iterations, one can obtain desired accuracies in the identification even with short data segments of measurements.

Next, we investigate the effect of assumption of the initial pdf $p(\boldsymbol{\theta}_0)$. In the absence of any information, $p(\boldsymbol{\theta}_0)$ is assumed to be uniformly distributed in the range $[a, b]$. Different choices

Copyright © 2000 John Wiley & Sons, Ltd.

Prepared using stcauth.cls

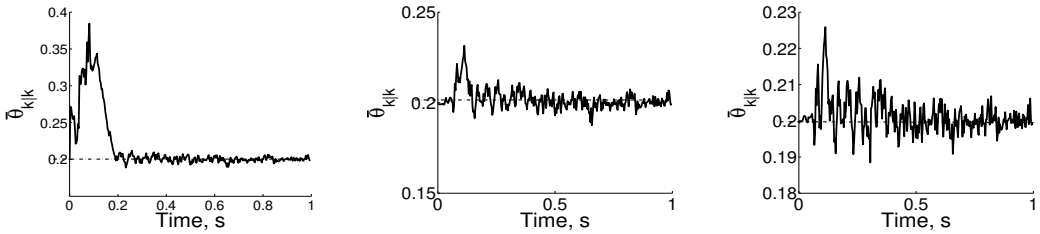

(a) Iteration 1 (b) Iteration 2 (c) Iteration 3

Figure 5: Estimates of the mean $\bar{a}$ with global iterations: actual crack size $\bar{a} = 0.2$.

of a and b are considered; the results are shown in Fig. 6 for the case $\bar{a} = 0.2$. Figure 6(a)

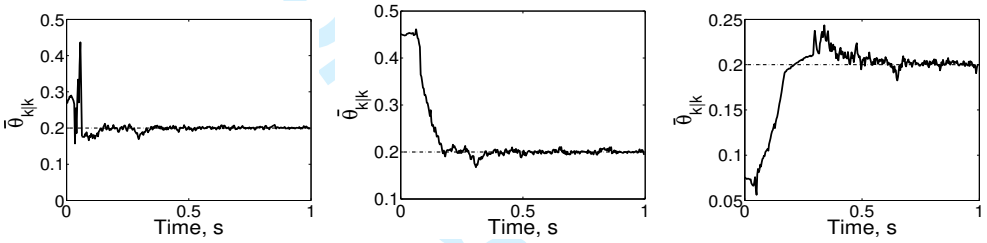

(a) $a = 0.05,\ b = 0.5$ (b) $a = 0.4,\ b = 0.5$ (c) $a = 0.05,\ b = 0.1$

Figure 6: Effect of assumption of initial pdf $p(\boldsymbol{\theta}_0)$ on the accuracy of the estimates.

considers the case where the range $(b - a)$ is large such that $\bar{a}$ lies within this range. In Fig. 6(b), a is much higher than $\bar{a}$ while in Fig. 6(e) b is much smaller than $\bar{a}$. Though in all cases, the estimates converged to the correct results, it is observed that when the range of $p(\boldsymbol{\theta}_0)$ encompasses the actual crack size $\bar{a} = 0.2$, faster convergence is achieved. Importantly, these results show that even a wrong assumption of $p(\boldsymbol{\theta}_0)$ leads to correctly identifying the crack size.

The noise associated with the model and the measurement equations are assumed to be Gaussian white noise; thus, $\mathbf{w}_k$ and $\mathbf{v}_k$ are represented as Gaussian i.i.d. variables having standard deviation of 5% of the response range. The implication of assuming the noise to be i.i.d. random variables is that the noise processes are assumed to be delta-correlated. Delta-correlated noise processes, also known as white noise processes, have infinite energy and in reality are physical impossibilities. However, the fluctuations in the noise usually occur at faster scales than the system response. Thus, in the time scales at which the response are observed/measured, it is reasonable to assume that the correlation lengths of the noise processes are infinitesimally small. Hence, the assumption of noise being modeled as delta-correlated processes in the time scales of structure response, is not unrealistic. The assumption of the pdf for the noise is somewhat arbitrary. Since Gaussian models for noise are in general, considered to be acceptable, an investigation is carried out to check the robustness of the method for varying intensities of the noise. As $\mathbf{w}_k$ is an artificial noise of small intensity, only the intensity for $\mathbf{v}_k$ is varied; see Fig. 7 for the results. As the noise intensity increases, the

Copyright © 2000 John Wiley & Sons, Ltd.

Prepared using stcauth.cls

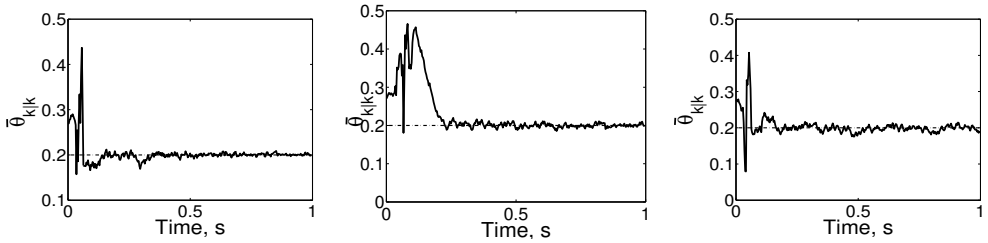

(a) $\mathbf{v}_k$ is 5% (b) $\mathbf{v}_k$ is 10% (c) $\mathbf{v}_k$ is 20%

Figure 7: Effect of assumption of noise intensity on the accuracy of the estimates.

accuracy of the estimates is observed to decrease. Here, one must recollect that $\mathbf{v}_k$ models the combined effect of the uncertainties in the measurements and in modeling the system. A high noise intensity implies that either the measurements are highly corrupted with noise, or the model for the system has gross inaccuracies, or both. In either case, it is unreasonable to expect accurate identification of the system parameters.

4.2. Identifying the crack size and location

We next show the usefulness of the proposed method in identifying the crack size as well as its approximate location. We take the same beam considered in the previous example. As before, the synthetic measurements are generated by numerically solving the forward problem and adding noise to the response. In solving the forward problem, the beam is modeled using finite elements discretized into 5 finite elements. The element containing the crack is modeled using the cracked beam element and the rest of the elements are modeled as Euler-Bernoulli beam elements. The synthesized response is taken to be the input to the particle filtering algorithm. However, in the finite element model used in the particle filtering algorithm, we use the cracked beam element for all the 5 elements. As an initial guess, the size of the cracks in each element is assumed to be equal *i.e.*, $\{\bar{a}_i\}_{i=1}^{5} = 0.2$. The proposed algorithm is now used to estimate the crack sizes in each of these elements. Thus, the dimension of the vector of system parameters to be identified, $\boldsymbol{\theta}$, is 5. If there exists only one predominant crack, it is expected that the estimates of 4 parameters in the vector $\boldsymbol{\theta}$ would converge to zero. The non-zero value in $\boldsymbol{\theta}$ not only gives an estimate of the crack size, but an approximate location can be determined from the location of the corresponding finite element with respect to the beam. In this problem, the crack has been first assumed to exist within the third element. Figure 8 illustrates the estimates of $\bar{a}_i$ at each of the i elements for 5 global iterations. It is observed that by the fifth iteration, estimates of $\bar{a}_3$, corresponding to the third element converge to the correct value, while the rest correctly converge to zero. The probability mass function for $\bar{a}_i$ in the 5 elements, at a particular time instant for iteration 2, is shown in Fig. 9. The mean values computed from each of these probability mass functions is the mean estimates that are shown in Fig. 8. The probability mass functions shown in Fig. 9 change at every instant the particle filter is employed. The samples that are generated to predict the response at the next time step are drawn from these mass functions. Since it was found from earlier studies that the estimates are reasonably accurate for crack sizes up to $\bar{a} = 0.025$, when the mean estimates become less than 0.025, they are forcibly made to be zero. This is done so as to avoid obtaining

Copyright © 2000 John Wiley & Sons, Ltd.

Prepared using stcauth.cls

For Peer Review

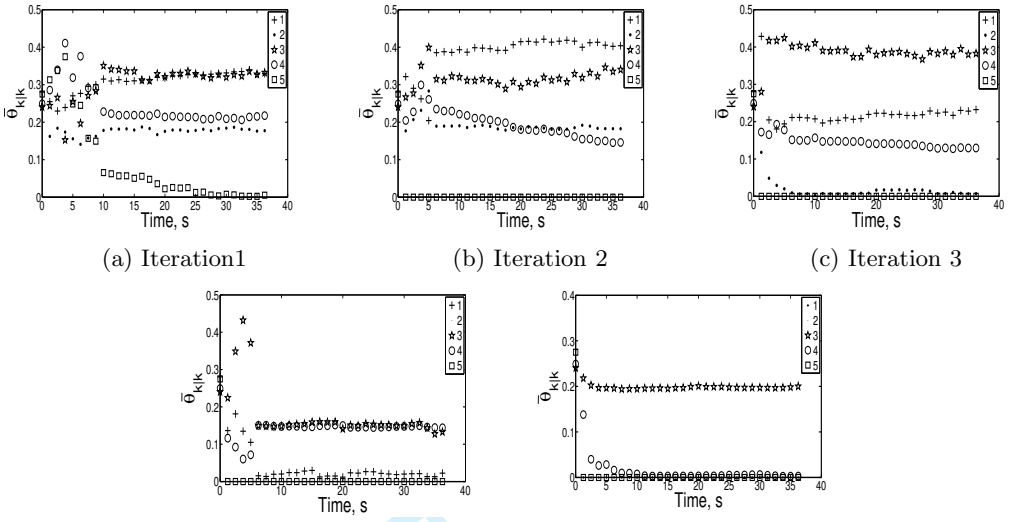

(a) Iteration1 (b) Iteration 2 (c) Iteration 3

(d) Iteration 4 (e) Iteration 5

Figure 8: Estimates of the crack size in the 5 elements.

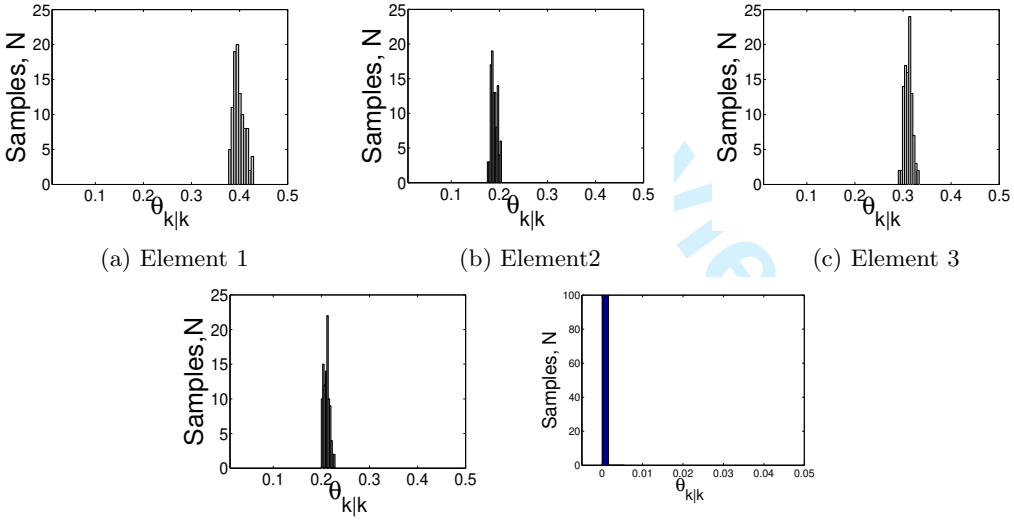

(a) Element 1 (b) Element2 (c) Element 3

(d) Element 4 (e) Element 5

Figure 9: The probability mass function for the crack size at $t = 10$s , in iteration 2.

Copyright © 2000 John Wiley & Sons, Ltd.

Prepared using stcauth.cls

impossible estimates of crack sizes, such as negative sizes. The possibility of obtaining negative crack sizes arise due to the effect of the artificial noise $\mathbf{w}_k$.

Figure 10 show the estimates of the crack size at the end of 3 global iterations, when the predominant crack is assumed to be in element 1, 2, 4 and 5 respectively. In all cases, the accelerations are measured at the tip of the beam (right end node of element 5). The actual crack size in each of these cases was taken to be $\bar{a} = 0.2$. Note that the estimates when the crack exists in element 3 has already been presented in Fig. 8. From the results shown in Fig. 10 it is observed that the predominant crack location and its size is reasonably identified by the third iteration.

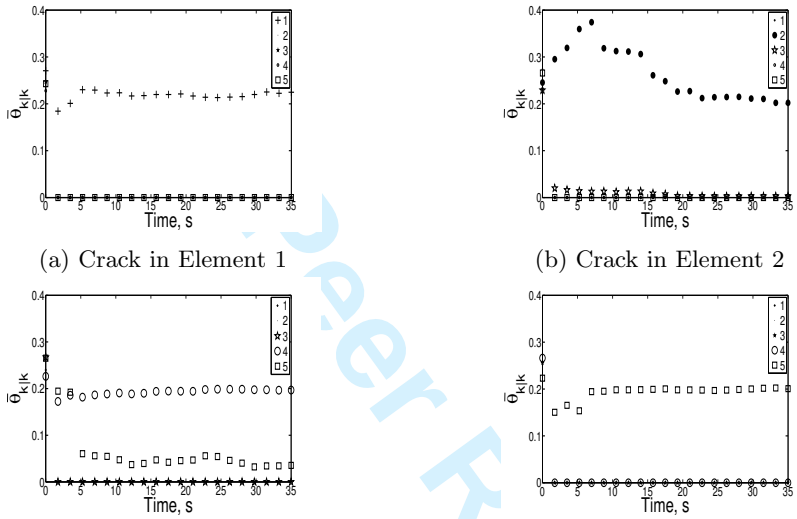

(a) Crack in Element 1 (b) Crack in Element 2

(c) Crack in Element 4 (d) Crack in Element 5

Figure 10: Estimated crack sizes at the third global iteration; measurements taken at the tip of the beam.

Next, studies are carried out to investigate the dependency of the accuracy of the algorithm and the locations where the response are measured. Here, it is assumed that the measurements are taken at the right end node of the third element. Four different cases are considered where the predominant crack is located at elements 1, 2, 4 and 5 respectively. Figure 11 illustrates the mean crack size for the four cases, at the third global iteration. It is observed that the algorithm is reasonably accurate in identifying the predominant crack size, though there appears to be a false detection of a crack, when there is a crack in element 4. The existence of false alarms can be avoided by executing the algorithm afresh, but by assuming cracks to exist only at the two elements where cracks have been identified. Importantly, it is observed that the algorithm is able to identify the crack irrespective of where the measurements are taken and based on only one set of response measurements.

Copyright © 2000 John Wiley & Sons, Ltd.

Prepared using stcauth.cls

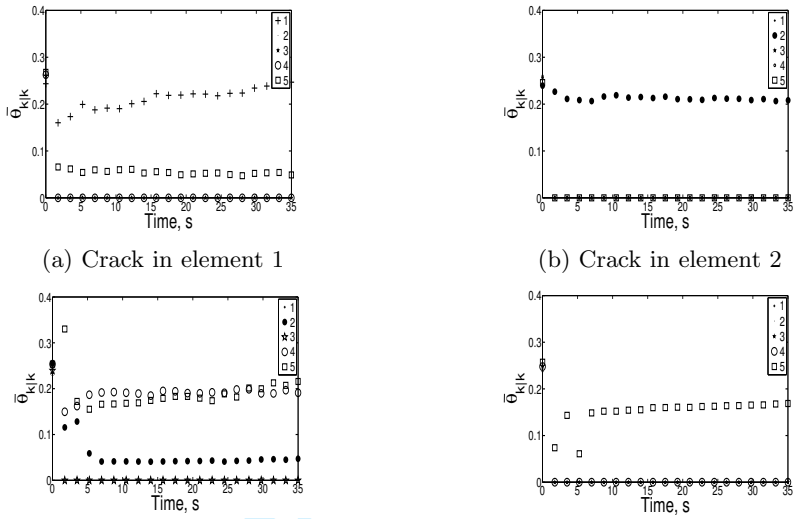

(a) Crack in element 1 (b) Crack in element 2

(c) Crack in element 4 (d) Crack in element 5

Figure 11: Estimated crack sizes at the third global iteration; measurements taken at right end node of third element.

5. Experimental Verification

This section investigates the applicability of the proposed method for identifying cracks using experimentally acquired measurements. A rectangular aluminium beam of length 310 mm and having cross-sectional dimensions of 25.65 mm× 3.25 mm is considered. The excitations were imparted through a V406 LDS electrodynamic shaker. The application of base vibrations with the shaker implied attaching the beam to the shaker directly. However, on account of

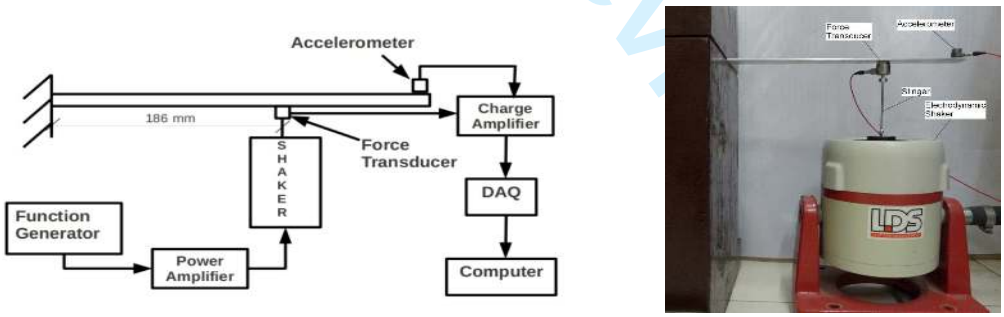

(a) Schematic diagram. (b) Photo of fixture

Figure 12: Experimental setup.

slight transverse rotations at the support lead to difficulties in mimicking the base excitations considered earlier in this paper. Instead, we imparted a concentrated load on the beam

Copyright © 2000 John Wiley & Sons, Ltd.

Prepared using stcauth.cls

through the shaker. The location of the point of excitation was taken to be 186 mm from the support, such that the location coincided with a midpoint of an element when the beam is mathematically modelled using a 5-element FE model. A Dytran force transducer with a sensitivity of 493.1 mV/lbf is placed at the point of excitation to measure the force imparted to the cantilever beam. A Dytran $3055B2$ accelerometer was placed at the tip of the beam to measure the tip accelerations of the response; see Fig. 12. Since the weight of the accelerometer (8.6 gms) was not negligible in comparison to the weight of the beam, the accelerometer was included in the FE model as a lumped mass at the tip. More details on the experimental set-up and studies on the corresponding mathematical models is available in [45]. A 16-channel NI 6341 USB data acquisition system was used to acquire the force and the tip accelerations of the beam over two channels. The sampling rate was kept at 1000 samples/s. These measurements are used as inputs to the particle filter algorithm.

A saw cut, across the breadth of the beam, was introduced into the beam at a location of 186 mm from the fixed end; see Fig. 13a for a close-up photo. The depth of the saw-cut, a, is

(a)

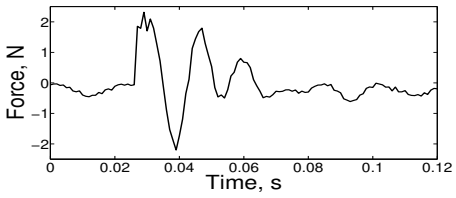

(b)

Figure 13: (a) Close-up photo of the saw-cut damage in the beam, (b) Time history of arbitrary force imparted to the beam.

measured using a crack depth gauge and the $\bar{a}$ is measured to be 0.3. It must be mentioned here that introducing a crack like defect in a beam is a complicated procedure. First, one needs to initiate a V-notch and subsequently, the sample needs to be subjected to repeated loadings in a fatigue testing machine. This can be time consuming and a complicated process. Instead, using a saw-cut as a crude model for a crack like defect is simpler. Moreover, it has been shown that the vibration characteristics of a beam with a saw-cut defect and a crack which always remain open are quite similar [46, 47]; the differences between the two cases become marked only when the cracks start propagating.

Next, an arbitrary forcing is imparted to the beam through the shaker; see Fig. 13b for the time history. The experimentally acquired measurements are now used as inputs to the particle filter. $\boldsymbol{\theta}$ is a 5-dimensional vector. $p(\boldsymbol{\theta}_0)$ are assumed to uniformly distributed in [0, 0.3] and N is taken to be 100. The estimates of $\bar{a}_i$ in the 5 elements, as a function of time, are shown in Figs. 14(a)-14(e). It is observed that at the end of iteration 5, the crack size in element 3 converges correctly to $\bar{a} = 0.3$. However, the fifth element also shows a convergence to a crack size of $\bar{a} \approx 0.1$. Clearly this is a false identification. We next consider a FE model where cracks are assumed to be available only in elements 3 and 5 and carry out particle filtering with the time history signals acquired earlier. Thus, $\boldsymbol{\theta}$ is now of dimension 2. $p(\boldsymbol{\theta}_0)$ is taken to be the probability mass functions for the corresponding elements obtained earlier at the end of iteration 5. Figures 15(a) -15(c) show the estimates of $\bar{a}$ for the two elements as a function of time and as the number of iterations increase. It is observed that the mean value for $\bar{a}$ at

Copyright © 2000 John Wiley & Sons, Ltd.

Prepared using stcauth.cls

For Peer Review

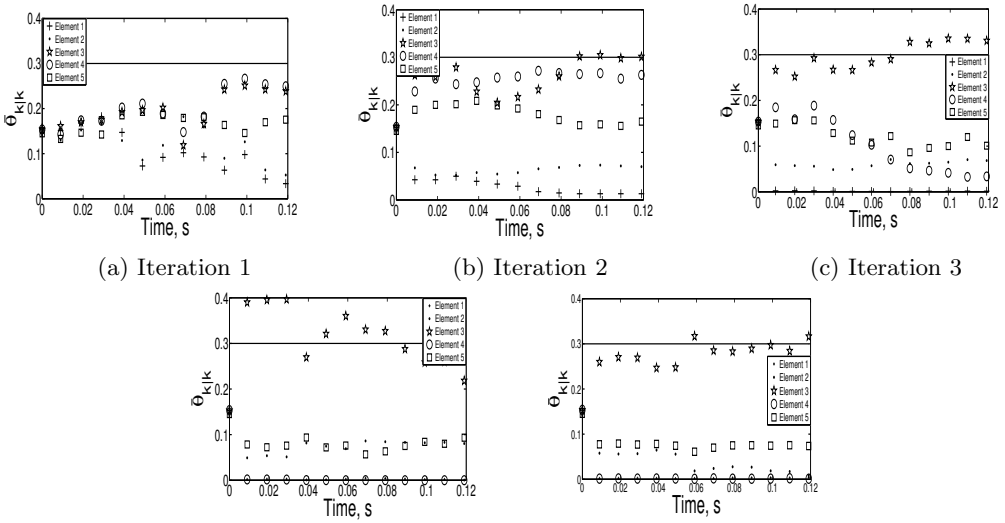

(a) Iteration 1 (b) Iteration 2 (c) Iteration 3

(d) Iteration 4 (e) Iteration 5

Figure 14: Estimates of the crack size in the 5 elements for arbitrary forcing.

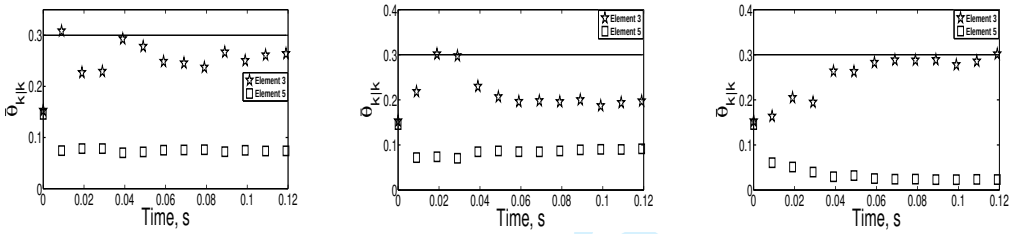

(a) Iteration 1 (b) Iteration 2 (c) Iteration 3

Figure 15: Estimates of the crack size in the 2 elements for arbitrary forcing.

the end of iteration 3 in element 3 is 0.302 indicating an error of 0.53%. The corresponding standard deviation of the estimate is computed to be 0.01, indicating convergence. The mean value of $\bar{a}$ in element 5 is 0.023 which is of the order of the noise levels and hence can be neglected.

The above two-step procedure gives an indication of how the method can be applied to large scale engineering structures. The key complexities include handling a larger dimension for $\boldsymbol{\theta}$ and a more complicated FE model. Rather than direct application of the proposed method which will be computationally expensive, one can adopt the following approach:

(1) A simple model for the structural system having few unknown parameters is first considered. Thus, for example, the flexural rigidity of the major component members could be assumed to be constant over the spatial domain and treated as the unknown variables. This would ensure that the dimension of $\boldsymbol{\theta}$ remains low and is not related to

Copyright © 2000 John Wiley & Sons, Ltd.

Prepared using stcauth.cls

the number of finite elements.

(2) A comparison of the estimated parameters for $\boldsymbol{\theta}$ using the proposed algorithm and the likely values of the same for an undamaged structure would provide indications as to the components which are likely to have cracks or other defects.

(3) A more sophisticated FE model could be created next with $\boldsymbol{\theta}$ comprising of parameters of the elements in the regions likely to have defects. The particle filtering can be carried out with respect to these parameters only.

There can be no prescriptive methods for application of these algorithms for large engineering structures. Combined with basic engineering knowledge and intelligent modelling of the system, one can use the proposed method for identifying crack like defects from vibration measurements. It must be noted that reductions in the computational costs is achieved at the price of accuracy of the estimates. Existing methods available in the literature require large data sets of vibration measurements which require large investments in sensor and data acquisition costs. In comparison, here the computational costs appear to be higher.

6. Concluding Remarks

The present study proposes a methodology for detection of breathing crack-like defects by estimating their size and location from vibration measurements using principles of dynamic state estimation. The methodology, by adapting the existing particle filter algorithms to the specific problem of crack-detection, has distinct advantages over conventional methods such as modal analysis and deterministic time domain based methods as it requires significantly lesser data to be acquired. The methodology was applied in detection of a nominal crack like defect in a vibrating cantilever beam. In the discretized finite element model of the beam, the effect of crack on the flexibility of beam elements was incorporated as per theory of elasto-plastic fracture mechanics under small scale yielding conditions. Based on the studies carried out, the following remarks can be made:

1. The proposed method is effective in detection of cracks even with vibration measurements available for a short interval of time and at a single location.
2. The effects of measurement noise and model noise, as long as the signal to noise ratio are within acceptable limits, are effectively handled and is not an impediment to the identification procedure. This is particularly important as typically vibration measurements are taken through accelerometers which invariably have significant noise.
3. The numerical implementation of the method shows it to be sensitive to small cracks with crack-depth ratios as small as 2.5%. Such accuracy, subject to corroboration from measurements from physical experiments, can prove to be very beneficial for non-destructive identification of cracks at their early stages of development. To the best of the authors' knowledge, existing modal analysis based methods for crack detection are not sensitive to such small crack sizes, even when only synthetic measurements are used.
4. Though the proposed method requires an initial guess for the pdf of the parameters to be identified, the numerical studies illustrate that a wrong assumption for the pdf does not adversely affect the identification. However, the computational costs are higher when the choice of the pdf is grossly erroneous.

Copyright © 2000 John Wiley & Sons, Ltd.

Prepared using stcauth.cls

For Peer Review

5. The estimates for the location of the damage is approximate and is primarily governed by the mesh size adopted in the FE model. For better accuracy of the estimates of the crack locations, one could either (a) adopt a finer mesh size but which will increase the computational costs at each filtering step, or (b) adopt an iterative approach where after the crack is identified within an element, filtering is carried out once more with a FE model where a finer meshing is adopted for the identified element only. Such iterative approaches is expected to reduce the possibilities of false alarms also.
6. The assumption of using breathing cracks is not restrictive in the context of the identification strategy. For cracks which close, open partially or fully during various stages of the vibration cycles, the flexibility parameter c would be a function of time. The identification of system parameters that are functions of time are akin to the state identification problems considered in the development of the particle filter in [42]. The difference would be in using appropriate nonlinear field equations in place of Eq. (1) and Eqs.(20-21). The concerns are similar if the cracks propagate during the acquisition of the measurements. As long as the physics of the problem is adequately modelled into the particle filter equations, no conceptual difficulties are expected in the application of the proposed identification algorithm.
7. Though it appears that the proposed method should be able to identify multiple cracks also, the reader is cautioned on this aspect. This is because the development of the FE cracked beam element considered the effects due to a single crack only. The presence of multiple cracks is expected to have interaction effects on each other and needs to be suitably modelled. The development of such finite elements is however beyond the scope of the present study.
8. The numerical examples considered only measurements from a single sensor. Using measurements obtained from multiple sensors is expected to increase the robustness of the identification algorithm [48]. In the context of the present study, the placement of additional sensors did not lead to improvement of results as long as a sensor was placed at the tip of the beam. More detailed studies on the placement of sensors within the context of the problem is required.
9. Minimization of the computational costs can be achieved if the proposed method is integrated with efficient sampling algorithms, such as, importance sampling, latin hypercube sampling etc. Alternative strategies for minimizing the computational costs associated with the bootstrap particle filter by transforming the forward problem into abstract mathematical space has been addressed in a separate study in [49] and is outside the scope of the present work.

Finally, a note of caution. Damage detection methods either require sufficiently reliable FE models for representing the undamaged state or measurements from the undamaged structure. In the latter approach, measurements are used to either bypass structure modelling or are used to update the FE model with which model based SHM techniques can be used. The proposed method requires a reasonably accurate FE model without the need for baseline measurements. Even though the formulation accounts for model errors, the predictions from a grossly inaccurate FE model may not be reliable. In such a case, one would need measurement data from the undamaged state. Genetic algorithm based studies [50,51] for crack identification also bypass the need for benchmark measurements of the undamaged structure. However, unlike these methods, the proposed method built on the principles of Bayesian filtering is

Copyright © 2000 John Wiley & Sons, Ltd.

Prepared using stcauth.cls

For Peer Review

shown to work well even with measurements with significant noise.

Acknowledgement

This work was partially supported from the project sponsored under the National Program on Micro and Smart Systems (NPMASS), Aeronautical Development Agency, Government of India.

REFERENCES

1. Farrar CR, Doebling SW, Nix DA. Vibration based structural damage identification. *Philosophical Transactions of Royal Society London A* 2001; **359**: 131-149.
2. Dimarogonas AD. Vibration of cracked structures: A state of the art review. *Engineering Fracture Mechanics* 1996; **55**(5): 831-857.
3. Lin HP. Direct and inverse methods on free vibration analysis of simply supported beams with a crack. *Engineering Structures* 2004; **26**: 427-436.
4. Cawley P, Adams RD. The locations of defects in structures from measurements of natural frequencies. *Journal of Strain Analysis* 1979; **14**: 49-57.
5. Ismail F, Ibrahim A, Martin HR. Identification of fatigue cracks from vibration testing. *Journal of Sound and Vibration* 1990; **40**(2): 305-317.
6. Ostachowicz WM, Krawczuk M. Analysis of the effect of cracks on the natural frequencies of a cantilever beam. *Journal of Sound and Vibration* 1991; **150**(2): 191-201.
7. Li QS. Vibratory characteristics of Timoshenko beams with arbitrary number of cracks. *Journal of Engineering Mechanics ASCE* 2003; **129**(11) : 1355-1359.
8. Shen MH, Taylor JE. An identification problem for vibrating cracked beams. *Journal of Sound and Vibration* 1991; **150** : 457484.
9. Armon D, Ben-Haim Y, Braun S. Crack detection in beams by rank-ordering of eigenfrequency shift. *Mechanical Systems and Signal Processing* 1994; **8**: 81-91.
10. Nandwana BP, Maiti SK. Modeling of vibration of beam in presence of inclined edge or internal crack for its possible detection based on frequency measurements. *Engineering Fracture Mechanics* 1997; **58** : 193-205.
11. Lee YS, Chung MJ. A study on crack detection using eigenfrequency test data. *Computers and Structures* 2000; **77** : 327-342.
12. Morassi A, Rollo M. Identification of two cracks in a simply supported beam from minimal frequency measurements. *Journal of Vibration Control* 2001; **7** : 729734.
13. Morassi A. Identification of a crack in a rod based on changes in a pair of natural frequencies. *Journal of Sound and Vibration* 2001; **242** : 577596.
14. Shim MB, Suh MW. A study on multiobjective optimization technique for inverse and crack identification problems. *Inverse Problems in Engineering* 2002; **10**: 441465.
15. Patil DP, Maiti SK. Detection of multiple cracks using frequency measurements. *Engineering Fracture Mechanics* 2003; **70** : 1553-1572.
16. Shim MB, Suh MW. Crack identification using evolutionary algorithms in parallel computing environment. *Journal of Sound and Vibration* 2003; **262** :141160.
17. Dharmaraju N, Tiwari R, Talukdar S. Development of a novel hybrid reduction scheme for identification of an open crack model in a beam. *Mechanical Systems and Signal Processing* 2005; **19**: 633-657.
18. Karthikeyan M, Tiwari R, Talukdar S. Development of a technique to locate and quantify a crack in a beam based on modal parameters. *Journal of Vibrations and Acoustics ASME* 2007; **129**: 390-395.
19. Karthikeyan M, Tiwari R, Talukdar S. Development of a novel algorithm for crack detection, localization and sizing in a beam based on forced response measurements. *Journal of Vibrations and Acoustics ASME* 2008; **130**: 021002.
20. Bamnios Y, Douka E, Trochidis A. Crack identification in beam structures using mechanical impedance. *Journal of Sound and Vibration* 2002; **256** : 287-297.
21. Dharmaraju N, Sinha JK. Some comments on use of antiresonance for crack identification in beams. *Journal of Sound and Vibration* 2005; **286** : 669-671.
22. Dilena M, Morassi A. The use of antiresonances for crack detection in beams. *Journal of Sound and Vibration* 2004; **276** (2004): 195-214.

Copyright © 2000 John Wiley & Sons, Ltd.

Prepared using stcauth.cls

For Peer Review

23. Rubio L. An efficient method for crack identification in simply supported Euler-Bernoulli beams. *Journal of Vibrations and Acoustics ASME* 2009; **131** : 051001.
24. Chang CC, Chen LW. Vibration damage detection of a Timoshenko beam by spatial wavelet based approach. *Applied Acoustics* 2003; **64** :1217-1240.
25. Li B, Chen XF, Ma JX, He ZH. Detection of crack location and size in structures using wavelet finite element methods. *Journal of Sound and Vibration* 2005; **285** : 767-782.
26. Cattarius J, Inman DJ. Time domain analysis for damage detection in smart structures. *Mechanical Systems and Signal Processing* 1997; **11** : 409423.
27. Koh CG, Hong B, Liaw CY. Parameter identification of large structural systems in time domain. *Journal of Structural Engineering ASCE* 2000; **126**: 957963.
28. Majumder L, Manohar CS. A time domain approach for damage detection in beam structures using vibration data with a moving oscillator as an excitation source. *Journal of Sound and Vibration* 2003; **268** : 699-716.
29. Majumder L, Manohar CS. Nonlinear reduced models for beam damage detection using data on moving oscillator-beam interactions. *Computers and Structures* 2004; **82** : 301-314.
30. Law SS, Lu ZR. Crack identification in beam from dynamic responses. *Journal of Sound and Vibration* 2005; **285**: 967-987.
31. Sinha JK, Friswell MI, Edwards S. Simplified models for the location of cracks in beam structures using measured vibration data. *Journal of Sound and Vibration* 2002; **251**: 13-38.
32. Kalman RE. A new approach to linear filtering and prediction problems. *Journal of Basic Engineering -D ASME* 1960; **82** : 35-45.
33. Hoshiya M, Saito E. Structural identification by extended Kalman filter. *Journal of Engineering Mechanics ASCE* 1984; **110** : 1757-1770.
34. Ghanem R, Shinozuka M. Structural system identification I. Theory. *Journal of Engineering Mechanics ASCE* 1995; **121** : 255-264.
35. Shinozuka M, Ghanem R. Structural system identification II: experimental verification. *Journal of Engineering Mechanics ASCE* 1995; **121** : 265-273.
36. Wang D, Haldar A. System identification with limited observations and without input. *Journal of Engineering Mechanics ASCE* 1997; **123** : 504-511.
37. Nasrellah HA, Manohar CS. Particle filters for structural system identification using multiple test and sensor data: a combined computational and experimental study. *Structural Control and Health Monitoring* 2001; **18** : 99-120.
38. Krawczuk M, Zak A, Ostachowicz W. Elastic beam finite element with a transverse elasto-plastic crack. *Finite Elements in Analysis and Design* 2000; **34** : 61-73.
39. Irwin GR. Plastic zone near a crack and fracture toughness. *Proceedings of Seventh Material Research Conference*, Syracuse University, Syracuse NY, 1960: 63-78.
40. Paris PC, Tada H, Irwin GR. *The stress analysis of cracks handbook.* Dell Research Corporation, Pennsylvania, 1973.
41. Rashid MF, Banerjee A. Implementation and validation of a triviality dependent cohesive zone model: experiments and simulation. *International Journal of Fracture* 2013; **181**: 227-239.
42. Gordon NJ, Salmond DJ, Smith AFM. Novel approach to nonlinear/non-Gaussian Bayesian state estimation. *IEE Proceedings* 1993; **140** : 107-113.
43. Nasrellah HA, Manohar CS. A particle approach for structural system identification in vehicle-structure interaction problems. *Journal of Sound and Vibration* 2010; **329** : 1289-1309.
44. Pokale, B. An experimental study on system identification in beams from vibration measurements. MS Thesis, Indian Institute of Technology Madras, 2013.
45. Pokale B, Gupta S. Damage estimation in vibrating beams from time domain experimental measurements. *Archive of Applied Mechanics* in press.
46. Gundmundson P. The dynamic behaviour of slender structures with cross-sectional cracks. *Journal of Mechanics Physics and Solids* 1983; **31** : 329-345.
47. Springer WT, Lawrence KL, Lawley TJ. Damage assessment based on the structural frequency-response function. *Journal of Experimental Mechanics* 1988; **28**: 34-37.
48. Mukhopadhyay S, Lus H, Betti R. Modal parameter based structural identification using inputoutput data: Minimal instrumentation and global identifiability issues. *Mechanical Systems and Signal Processing* 2014; **45**: 283301.
49. Rangaraj P, Chaudhuri A, Gupta S. The use of polynomial chaos for parameter identification from measurements in nonlinear dynamical systems. *ZAMM*, in press.
50. Rabinovich D, Givoli D, Vigdergauz S. XFEM-based crack detection scheme using a genetic algorithm. *International Journal for Numerical Methods in Engineering* 2007; **71**:10511080.
51. Chatzi EN, Hiriyur B, Waisman H, Smyth A. Experimental application and enhancement of the XFEM-GA algorithm for the detection of flaws in structures. *Computers & Structures* 2011; **89**:556570.

Copyright © 2000 John Wiley & Sons, Ltd.

Prepared using stcauth.cls

For Peer Review